EFFECTS OF GEOMETRIC PARAMETERS ON FLUID-FLOW AND HEAT TRANSFER IN MICRO-CHANNEL HEAT SINK WITH TRAPEZOIDAL GROOVES IN SIDEWALLS

by

Qifeng ZHU**, Feiyue ZHU, Dianwei FU, Anchao ZHANG, and Sen ZHANG

School of Mechanical and Power Engineering, Henan Polytechnic University, Jiaozuo, China

Original scientific paper
https://doi.org/10.2298/TSCI220129049Z

Trapezoidal grooves were arranged in channel sidewalls of the proposed micro-channel heat sinks to enhance heat transfer for cooling microelectronic systems. The 3-D numerical simulations were carried out to investigate the characteristics of fluid-flow and heat transfer in the proposed micro-channels. Field structures of thermal fluid-flow, Nusselt number, and friction factor, f, were employed to study the effects of the relative groove depth, α, and relative grooves spacing length, β, of trapezoidal grooves on the thermal and hydraulic performance of the proposed micro-channels. The results showed that the proposed micro-channel presented better flow and thermal performance than the smooth straight one for Re <597.74 with $f/f_0 < 1$ *and for Re >149.44 with* $Nu/Nu_0 > 1$*, respectively. The thermal enhancement factor, η, was achieved up to 1.197 with α = 0.4 and β = 1 for Re = 714.18. Furthermore, the relative groove depth had much more significant influence on the overall performance than the relative groove spacing length.*

Key words: *heat transfer, micro-channel heat sink, numerical simulation, thermal enhancement, trapezoidal grooves*

Introduction

With the rapid increase of heat flux in microelectronic systems, cooling has become a key restriction for the progress of microelectronics industry. First proposed in 1980's, micro-channel heat sink [1] was used to remove the heat from electronic devices and maintain their performance in all conditions. Due to the high cooling efficiency with a small volume, micro-channel heat sinks have received a lot of attention from many researchers [2].

Based on the straight smooth micro-channel, effects of aspect ratio and hydraulic diameter on the thermal-hydraulic characteristics in micro-channels were conducted and it was found that the hydraulic diameter had much more significant effect on heat transfer enhancement than aspect ratio [3, 4]. Furthermore, the cross-section of channel was then changed to triangle and trapezoid for providing better thermal-hydraulic performance [5]. Recently, with the widely use of nanofluid in common heat exchangers, the deionized water was replaced with nanofluid as coolants in micro-channel heat sinks [6, 7], such as ZnO-water, TiO_2-water, Al_2O_3-water, *et al.* However, the smooth straight micro-channel cannot enhance heat transfer significantly due to the lack of high level flow disturbance in channels. To strengthen the fluid mixing in channels, many innovative designs of micro-channel heat sinks were proposed with better thermal-hydraulic performances than the smooth one [8], such as secondary channels

* Corresponding author, e-mail: zhuqifeng0811@163.com

[9, 10], channel curvature [11, 12], dimples and protrusions [13, 14], ribs [15-18], and grooves [19-25]. Among these innovative designs, the micro-channel with ribs can generate a significant thermal enhancement due to the strengthened flow disturbance in channels [15-18]. Unfortunately, the pressure drop of fluid through channels was also very large at higher Reynolds number and thus gradually lost its advantage as an effective technique to enhance heat transfer.

Due to the large pressure drop penalty of micro-channels induced by ribs, grooves are employed for micro-channels to enhance heat transfer with a lower pressure drop [19-25]. Grooves can enhance heat transfer through interrupting and redeveloping the thermal boundary-layers. Triangular grooves were first employed and can enhance heat transfer in micro-channel heat sinks [19]. Ahmed and Ahmed [20] indicated that the micro-channel with trapezoidal grooves had better thermal enhancement than that with rectangular or triangular grooves. Zhu *et al.* [22] compared the effects of triangular, trapezoidal, rectangular and fan-shaped grooves on the thermal-hydraulic characteristics in micro-channels. Kumar [23] found that the trapezoidal micro-channel with semi-circular grooves showed better heat transfer than the rectangular grooved-micro-channels. Based on trapezoidal grooves, Datta *et al.* [24] proposed a micro-channel heat sink with the combination of grooves and ribs and found that the combination of trapezoidal grooves and diamond ribs showed the best overall performance.

From the aforementioned literature discussion, micro-channel heat sinks with trapezoidal grooves had shown superior thermal enhancement. However, the trapezoidal grooves of various geometric parameters were seldom reported and it is still unknown which trapezoidal configuration is more suitable for micro-channel heat sinks. Therefore, the aim of this study is to explore the effects of geometric parameters of trapezoidal grooves in channel sidewalls on the thermal-hydraulic performance of grooved micro-channel heat sinks and find a geometric configuration of micro-channel heat sink with trapezoidal grooves that provides the best overall performance.

Geometric model of micro-channel heat sink

In present study, isosceles trapezoidal grooves were arranged in the sidewalls of the parallel channels in the proposed micro-channel heat sink. Due to the channels symmetry, a single unit of micro-channel heat sink was employed the computational domain for numerical simulations. Figure 1 illustrates the computational domain and geometric parameters of the

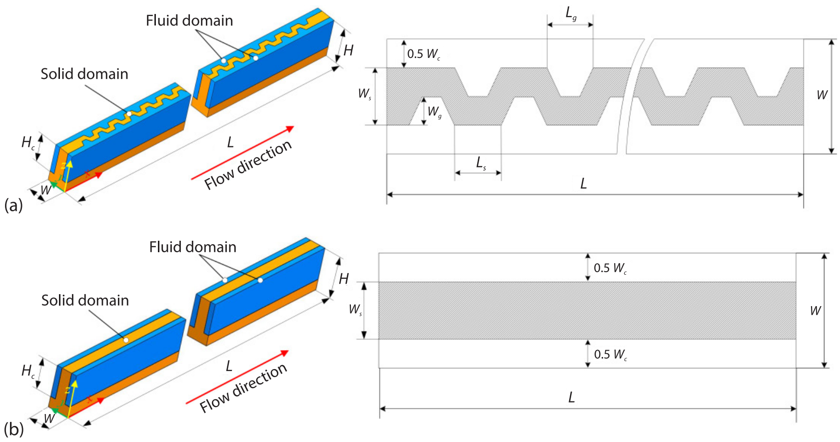

Figure 1. Schematic diagrams of computational domain and geometric parameters for; (a) micro-channel with trapezoidal grooves and (b) smooth straight micro-channel

proposed micro-channel and the corresponding smooth straight micro-channel. The main dimensions include the overall length, L, of 5 mm, the width, W, of 0.2 mm, and the height, H, of 0.4 mm. The channel height, H_c, is 0.3 mm and its width, W_c, is 0.1 mm, which is separated into two halves. The thickness, W_s, of the wall between two adjacent channels is 0.1 mm. The length, L_g, of trapezoidal grooves is 0.1 mm and other geometric parameters such as the groove depth, W_g, and the grooves spacing length, L_s, can be generated from two variables: one variable is the relative groove depth ($\alpha = W_g/L_g$) ranging from 0.1-0.5. The other variable is the relative grooves spacing length ($\beta = L_s/L_g$) ranging from 0.5-1.5.

Model description

Boundary conditions and numerical method

In present study, some basic assumptions are made to simplify the numerical calculation: the laminar and incompressible flow is in micro-channels [12, 14, 15, 18, 19]. The viscous dissipation, radiation heat transfer and surface tension are ignored [20-25]. The deionized water was employed as the working fluid and its thermophysical properties vary with temperature in accordance to the [25]. Silicon was employed as the solid material of micro-channel heat sink due to its relatively mature corrosion processing method and its good heat-conducting property. The density and the thermal conductivity of silicon are 2328.2 kg/m^3 and 148 W/(m·K), respectively. Qu and Mudawar [26] pointed out that the traditional N-S equation was still applicable when the channel diameter was larger than 0.1 mm and the Reynolds number was less than 1700. Velocity-inlet boundary was applied at the micro-channel inlet (x = 0 mm) with T_{in} = 293.15 K and u_{in} of 1 m/s, 2 m/s, 3 m/s, 4 m/s, and 5m/s corresponding to the Reynolds number of 149.44, 298.87, 448.31, 597.74, and 714.18, respectively. Pressure-outlet boundary was applied at channel outlet (x = 5 mm) with p_{out} = 0 Pa. The fluid-solid interfaces were defined as coupling walls with the fluid velocity of 0 m/s and the same temperature for both the fluid and solid, through which the heat was transported from the solid to the fluid-flowing in channels. The bottom surface of the geometric model was defined as heating surface with a constant heat flux $q = 10^6$ W/m^2. The two side surfaces of the computational domain (y = 0 mm and y = 0.2 mm) were defined as symmetry boundaries. Finally, the other surfaces were set as adiabatic boundaries.

The numerical simulations were conducted with the commercial software ANSYS FLUENT 14.5. The finite volume method was employed to discretize the governing equations with second order upwind scheme. Pressure-velocity coupling was accomplished using the SIMPLIC algorithm. To maintain the convergence of numerical simulations, the residual criterions were set to be 10^{-6} for all variables.

Grid independence test

The computational grid was generated by the GAMBIT 2.4 software. To save the computational cost, a grid independence test was implemented for present numerical simulations to find the optimal grid with a reasonable accuracy. The grids with cells number of 0.106 million, 0.352 million, and 0.736 million were chosen to be compared with that of 1.12 million for Re = 448.31. The relative error of pressure drop was expressed:

$$e\% = \left|\frac{M_2 - M_1}{M_1}\right| \times 100 \tag{1}$$

where M_1 represents the pressure drop obtained from the grid with 1.12 million cells while M_2 represents the results from other grids. The maximum error was 3.1%, 0.8%, and 0.6% corresponding to the grid with cells of 0.106 million, 0.352 million, and 0.736 million, respectively. Therefore, the grid with 0.352 million cells can be used for numerical simulations in present work.

Data acquisition

The Reynolds number is given:

$$\mathrm{Re} = \frac{\rho_\mathrm{f} u_\mathrm{in} D_\mathrm{h}}{\mu_\mathrm{f}} \tag{2}$$

where ρ_f and μ_f are, respectively, the density and dynamic viscosity of the fluid, u_in – the fluid velocity at channel inlet, and D_h – the channel hydraulic diameter and its expression can be given:

$$D_\mathrm{h} = \frac{2H_c \times W_c}{H_c + W_c} \tag{3}$$

The apparent friction factor is expressed:

$$f = \frac{\Delta p D_\mathrm{h}}{\rho_\mathrm{f} L u_\mathrm{in}^2} \tag{4}$$

where Δp is the pressure drop with its expression of $\Delta p = p_\mathrm{in} - p_\mathrm{out}$, p_in and p_out are, respectively the volume-based average pressure of inlet and outlet.

The heat transfer coefficient and Nusselt number:

$$h = \frac{q A_\mathrm{w}}{A_\mathrm{con}\left(T_\mathrm{w} - T_\mathrm{f}\right)} \tag{5}$$

$$\mathrm{Nu} = \frac{h D_\mathrm{h}}{k_\mathrm{f}} \tag{6}$$

where A_w is the heating surface area, A_con – the convection heat transfer area of fluid-solid interfaces, T_f – the fluid temperature, and k_f – the fluid thermal conductivity. The T_w and q represent the average area-weighted temperature and the constant heat flux of the heating surface, respectively.

The overall performance of the micro-channels can be evaluated using thermal enhancement factor, η. The η represents the overall performance of micro-channel heat sinks in terms of heat transfer and pumping power. The larger the thermal enhancement factor, the better the overall performance of micro-channel heat sinks. The expression of η is given [27]:

$$\eta = \frac{\mathrm{Nu}/\mathrm{Nu}_0}{\left(f / f_0\right)^{1/3}} \tag{7}$$

where subscript 0 is the smooth straight micro-channel, thus $\mathrm{Nu}/\mathrm{Nu}_0$ represents the relative average Nusselt number while f/f_0 represents the relative friction factor of the proposed micro-channel corresponding to the smooth straight channel.

Validation of numerical simulation

The validation of the present numerical simulation was conducted by comparing the numerical results with theoretical results. The pressure drop, Δp, and local Nusselt number, Nu_x, of the smooth straight micro-channel were employed for the comparison. The theoretical expressions of Δp and Nu_x were presented by Steinke *et al.* [28] and Phillips [29], respectively. Furthermore, a comparison of present numerical results with experimental results has also been made to validate the numerical model in our present study. The experimental results of Poiseuille number, *f*Re, and the average Nusselt number, $\overline{\mathrm{Nu}}$, for the smooth straight micro-channel are obtained from [30], hence, the present numerical simulations were performed with the same geometry and boundary conditions as that in [30]. Figure 2 shows the comparisons of the present numerical results with the theoretical data and experimental results. It is clearly shown that the present numerical results are in good agreement with that from theory method and the experimental results from [30]. As a result, the present simulations can be used to predict the thermal-hydraulic characteristics in the proposed micro-channels with trapezoidal grooves in channel sidewalls.

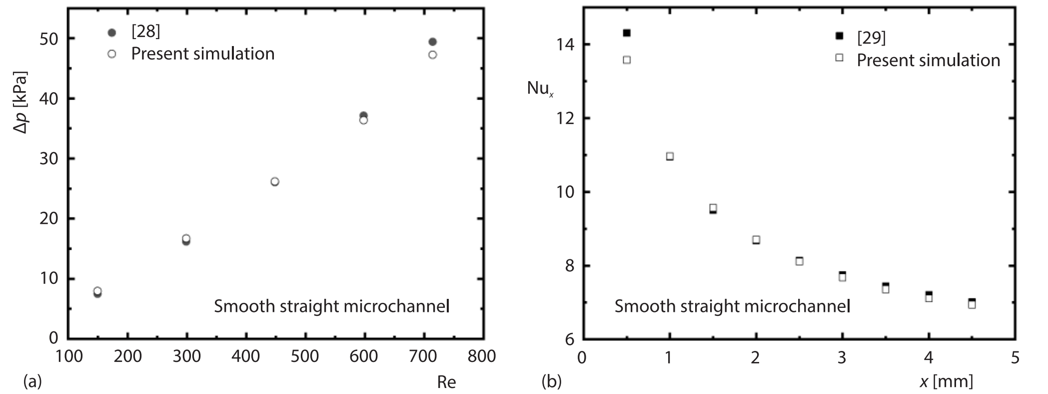

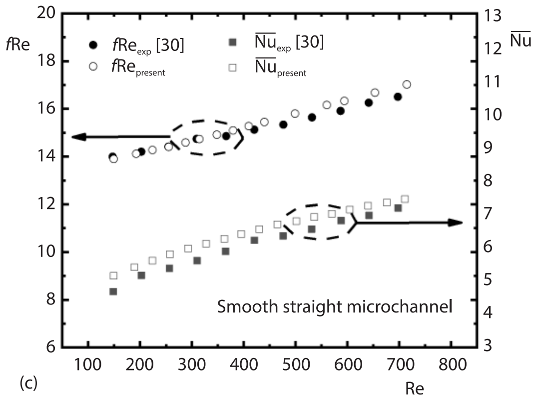

Figure 2. Comparisons of present numerical results with; (a) theoretical pressure drop, (b) theoretical local Nu_x, and (c) experimental results of Poiseuille number and average $\overline{\mathrm{Nu}}$ for the smooth straight micro-channel

Results and discussions

Effects of relative groove depth α

Effects of α on velocity distribution and streamlines in micro-channels

Figure 3 displays the velocity distribution and streamlines in the proposed micro-channels on the *x-y* plane of z = 0.2 mm with x in range of 2.4-3 mm at β = 1 for Re = 448.31. The flow boundary-layers were periodically interrupted by the grooves and redeveloped. It clearly shown that the fluid was separated into two parts, one part flowed into the grooves and formed vortexes for α > 0.1 due to the pressure gradient induced from the grooves; the other part flowed over the vortexes as the main flow fluid. These vortexes seemed as rolling bearings between the main flow fluid and the grooves walls, which may transform the sliding friction into rolling friction, thereby reducing the frictional resistance.

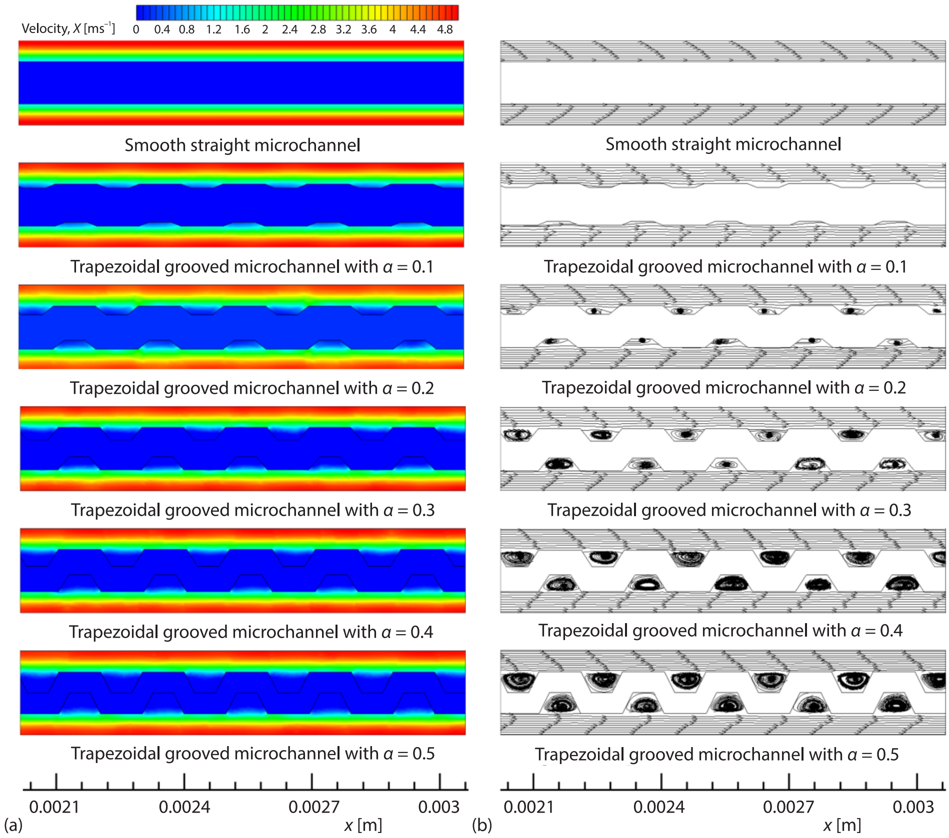

Figure 3. Effects of α on: (a) velocity distribution and (b) streamlines in micro-channels

Effects of α on temperature distribution

Figure 4 displays the temperature distribution on the x-y plane of z = 0.2 mm with x in range of 3-5 mm at β = 1 for Re = 448.31. The thermal boundary-layers of the proposed micro-channels with trapezoidal grooves were also interrupted and redeveloped periodically due to the grooves, which would improve the heat transfer performance. Therefore, all the micro-channels with trapezoidal grooves shows lower temperature than the smooth straight one. Among all the trapezoidal grooved micro-channels, the one with α = 0.1 has the highest temperature, followed by the one with α = 0.5, α = 0.3, α = 0.2 and α = 0.4, respectively. It clearly showed that the trapezoidal grooved micro-channel with α = 0.4 presents the lowest temperature among all the micro-channels, indicating that it may be the optimal design of trapezoidal grooves for the proposed micro-channel that has the best thermal performance.

Effects of α on thermal-hydraulic performance

Figure 5 illustrates the effects of α on the thermal-hydraulic performance of the micro-channel heat sinks at β = 1. As shown in fig. 5(a), the relative friction factor f/f_0 are less than 1 for Re < 597.74, indicating that trapezoidal grooves can reduce the flow resistance in the grooved micro-channels compared with the smooth one. For example, as α = 0.5 and Re = 149.44, the relative friction factor can be decreased down to 0.895 times lower than that of the smooth one. When α remains constant, the f/f_0 increases significantly with the increasing Reynolds number due to the enhanced flow disturbance in channels induced by the increased fluid velocity, indicating that the flow performance was significantly worsened due to the increase of fluid velocity for all cases.

Figure 5(b) displays the variation of Nu/Nu_0 with α for different Reynolds numbers. The average Nusselt numbers of all proposed trapezoidal grooved micro-channels are larger than that of the smooth straight one except for α = 0.1 and α = 0.5 at Re = 149.44. It can be explained that the flow disturbances in this two micro-channels were weaker at lower Reynolds numbers due to the lower fluid velocities, furthermore, the flow stagnation zones in the micro-channel with α = 0.5 are larger than other grooved micro-channels, which are negative for heat transfer. Overall, the micro-channels with trapezoidal grooves can generate better heat transfer performance for Re >149.44, compared with the smooth straight micro-channel. At α = 0.4 and Re = 714.18, the relative Nusselt number can be achieved up to 1.21 times higher than that of the smooth straight one. When α remains constant, the relative Nusselt number increases with the increasing Re, indicating that the heat transfer in the trapezoidal grooved micro-channels can be remarkably enhanced by increasing the flow velocity for present cases.

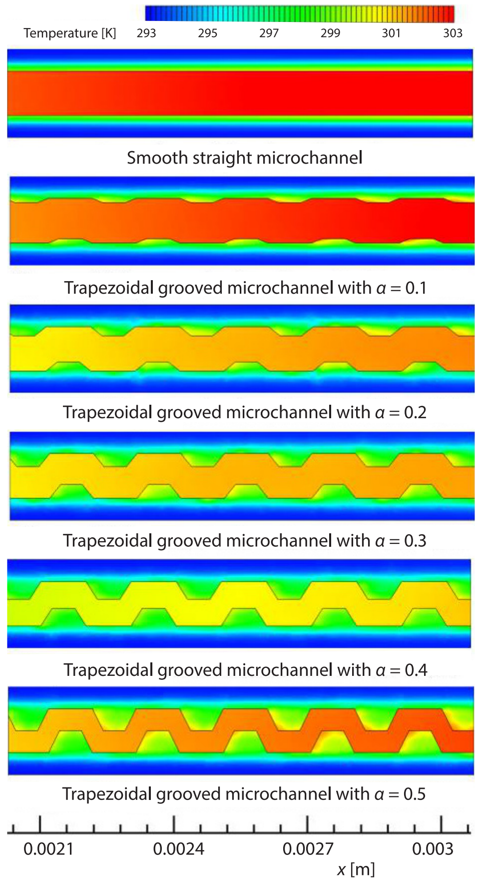

Figure 4. Effects of α on temperature distribution in micro-channels

Figure 5(c) shows the average temperature of the heating surface along the flow direction at Re = 448.31 and β = 1. All the micro-channels with trapezoidal grooves presented heat transfer enhancement with a lower temperature than that of the smooth straight one. Furthermore, the temperature difference between the proposed micro-channels gradually increased along the flow direction and the trapezoidal grooved micro-channel with α = 0.4 had the lowest temperature and the best thermal performance.

Figure 5(d) displays the variation of thermal enhancement factor η with α at β = 1. Although there is a smaller increasing rate for the micro-channel with α = 0.4 at higher Reynolds numbers, the thermal enhancement factor goes up steadily with the increase of Reynolds number. The thermal enhancement factors of the micro-channels with trapezoidal grooves are all larger than one for all cases, indicating that the comprehensive performance of micro-channel heat sink can be improved by arranging trapezoidal grooves in channel sidewalls. The trapezoidal grooved micro-channel with α = 0.4 has the largest thermal enhancement factor among all the micro-channels and its maximum can be achieved up to 1.197 for Re = 714.18.

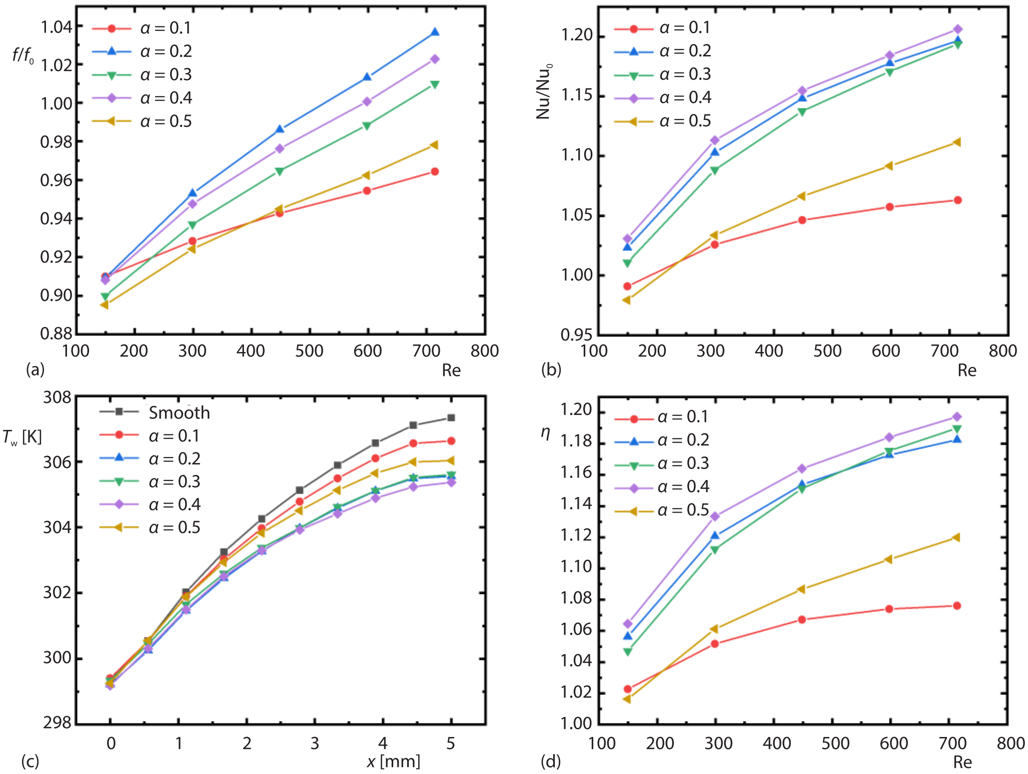

Figure 5. Effects of α on thermal-hydraulic performance for the micro-channels at β = 1

Effects of relative groove spacing length α

Figure 6 illustrates the effects of β on the thermal-hydraulic performance of the micro-channel heat sinks at α = 0.4. As shown in fig. 6(a), the present micro-channels with trapezoidal grooves had the relative friction factor f/f_0 less than 1 for Re < 597.74, indicating that the flow resistance was reduced compared with the smooth one. At β = 0.5 and Re = 149.44, the relative friction factor can decrease to 0.856 times lower than that of the smooth one. Furthermore, there is a drop of f/f_0 when β increases from 0.5-0.75 for Re = 597.74 and Re = 714.18. For other cases, f/f_0 increases with the increase of β due to the decrease of grooves, which reduces the channel volume, increases the fluid velocity and thereby increases the flow resistance in channels.

Figure 6(b) shows the variation of the relative Nusselt number Nu/Nu_0 with β for different Reynolds numbers at α = 0.4. The average Nusselt number of all trapezoidal grooved micro-channels are all larger than that of the smooth straight one except for β = 0.5 and β = 0.75 at Re = 149.44, which indicates that the micro-channels with trapezoidal grooves have superior thermal performance to the smooth one for Re >149.44 or β > 0.75. Furthermore, the maximum of Nu/Nu_0 can be achieved up to 1.21 for the micro-channel with trapezoidal grooves at β = 1 and Re = 714.18.

The heating surface temperature is important for the operation safety of electronic devices. The lower the temperature, the better the operation safety. Figure 6(c) displays the area averaged temperature of the heating surface along the flow direction at α = 0.4 for Re = 448.31.

The micro-channels with trapezoidal grooves showed a significant lower temperature of the heating surface than the smooth one, indicating that the heat transfer performance is enhanced. It should be noted that the maximal temperature difference between different β is less than 1 °C, suggesting that the spacing between the two adjacent grooves has little effect on heat transfer in the proposed micro-channels.

Figure 6(d) displays the effect of β on the thermal enhancement factor η. The variation of η presents the similar tendency to the variation of Nu/Nu_0 as shown in fig. 6(b). It can be clearly seen that the maximum of η generally appears at $\beta = 1$ for different Reynolds numbers while the minimum appears at $\beta = 0.75$. Furthermore, the maximum of η can be achieved up to 1.197 for the micro-channel with trapezoidal grooves at $\beta = 1$ and Re = 714.18. In particular, the maximal difference is 0.054 for β with the same Reynolds number, indicating that the relative grooves spacing length had less effect on the overall performance than relative groove depth for micro-channels.

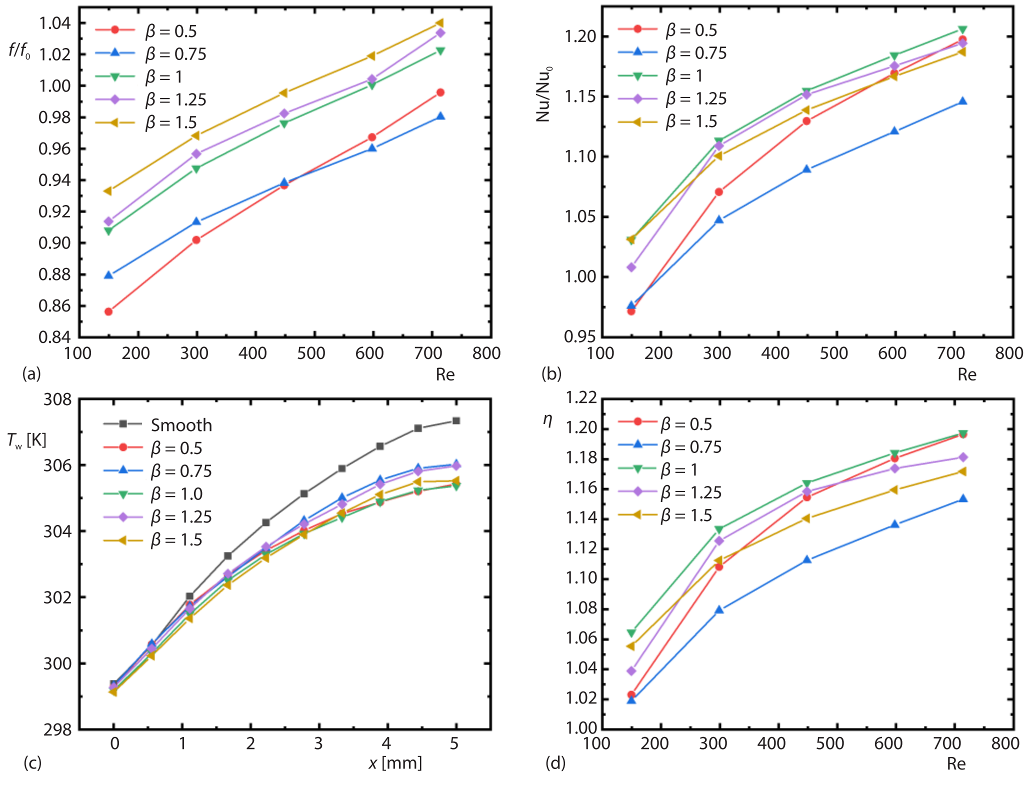

Figure 6. Effects of β on thermal-hydraulic performance for the micro-channels at α = 0.4

Conclusions

The major conclusions are summarized as follows.

- Vortexes were induced by grooves appearing as rolling bearings between the main flow fluid and grooves walls.
- The micro-channel with trapezoidal grooves had a lower apparent friction factor for Re < 500 and a higher average Nusselt number for Re > 150 compared with the smooth micro-channel.

- The proposed micro-channel heat sinks with trapezoidal grooves presented the best overall performance with η of 1.197 at $\alpha = 0.4$ and $\beta = 1$.
- The geometric parameter of α had much more significant influence on the overall performance than that of β.

Nomenclature

D_h – hydraulic diameter, [mm]
D_p – pressure drop, [Pa]
e – relative error of results
f – friction factor
f/f_0 – relative friction factor
H – height of computational domain, [mm]
H_c – height of fluid channel, [mm]
h – heat transfer coefficient, [$Wm^{-2}K^{-1}$]
k – thermal conductivity, [$Wm^{-1}K^{-1}$]
L – length of computational domain, [mm]
L_g – length of trapezoidal groove, [mm]
L_s – grooves spacing length, [mm]
M – performance parameter
Nu – Nusselt number
$\overline{\text{Nu}}$ – average Nusselt number
Nu_x – local Nusselt number
Nu/Nu_0 – relative Nusselt number
p – pressure, [Pa]
q – heat flux, [Wm^{-2}]
Re – Reynolds number
T – temperature, [K]
u – average velocity, [ms^{-1}]
x – x-axis, [mm]
y – y-axis, [mm]
z – z-axis, [mm]
W – width of computational domain, [mm]
W_s – width of the micro-channel, [mm]
W_c – width of solid fin, [mm]
W_g – width of trapezoidal groove, [mm]

Greek symbols

α – telative groove depth
β – relative grooves spacing length
η – thermal enhancement factor
μ – dynamic viscosity, [Pa·s]
ρ – density, [kgm^{-3}]

Subscripts

con – fluid-solid intersurfaces
f – fluid
in – inlet
s – solid
out – outlet
w – heating surface
0 – smooth straight micro-channel
1 – finest grid
2 – other grid

Acknowledgment

This study was supported by three programs of Henan Province in China, including the Program of Science and Technology (No. 212102210001), College Students' Innovative Entrepreneurial Training Plan Program (No. 202010460022) Program of Basic Education Research (No. 15A470002), and Technology Program for Coal Mine Safety Production (No. HN15-61).

References

[1] Tuckerman, D. B., Pease, R. F. W., High-Performance Heat Sinking for VLSI, *IEEE Electron Dev. Lett*, *2* (1981), 5, pp. 126-129
[2] Zhang, Z. Q., *et al.*, Thermal Management and Temperature Uniformity Enhancement of Electronic Devices by Micro Heat Sinks: A Review, *Energy*, *216* (2021), Feb., ID119223
[3] Sahar, A. M., *et al.*, Effect of Hydraulic Diameter and Aspect Ratio on Single Phase Flow and Heat Transfer in a Rectangular Micro-Channel, *Appl. Therm. Eng.*, *115* (2017), Mar., pp. 793-814
[4] Kou, H. S., *et al.*, Optimum Thermal Performance of Micro-Channel Heat Sink by Adjusting Channel Width and Height, *Int. Commun. Heat Mass Transf.*, *35* (2008), 5, pp. 577-582
[5] Gunnasegaran, P., *et al.*, The Effect of Geometrical Parameters on Heat Transfer Characteristics of Micro-Channels Heat Sink with Different Shapes, *Int. Commun. Heat Mass Transf.*, *37* (2010), 8, pp. 1078-1086
[6] Tran, N., *et al.*,. Optimization of Thermal Performance of Multi-Nozzle Trapezoidal Micro-Channel Heat Sinks by Using Nanofluids of Al_2O_3 and TiO_2, *Int. J. Heat Mass Transf.*, *117* (2018), Feb., pp. 787-798
[7] Narankhishig, Z., *et al.*, Convective Heat Transfer Characteristics of Nanofluids Including the Magnetic Effect on Heat Transfer Enhancement - A Review, *Appl. Therm. Eng.*, *193* (2021), July, ID116987

[8] Sidik, N. A. C., *et al.*, An Overview of Passive Techniques for Heat Transfer Augmentation in Micro-Channel Heat Sink, *Int. Commun. Heat Mass Transf.*, *88* (2017), Nov., pp. 74-83
[9] Shi, X. J., *et al.*, Geometry Parameters Optimization for a Micro-Channel Heat Sink with Secondary Flow Channel, *Int. Commun. Heat Mass Transf., 104* (2019), May, pp. 89-100
[10] Japar, W. M. A. A., N.A.C., *et al.*, A Comprehensive Study on Heat Transfer Enhancement in Micro-Channel Heat Sink with Secondary Channel, *Int. Commun. Heat Mass Transf.*, *99* (2018), Dec., pp. 62-81
[11] Sui, Y., *et al.*, Fluid-Flow and Heat Transfer in Wavy Micro-channels, *Int. J. Heat Mass Transf.*, *53* (2010), 13, pp. 2760-2772
[12] Ma, D. D., *et al.*, Effects of Structural Parameters on Fluid-flow and Heat Transfer Characteristics in Micro-Channel with Offset Zigzag Grooves in Sidewall, *Int. J. Heat Mass Transf.*, *101* (2016), Oct., pp. 427-435
[13] Li, M., *et al.*, Investigation of Flow Structure and Heat Transfer Enhancement in Rectangular Channels with Dimples and Protrusions Using Large Eddy Simulation, *Int. J. Therm. Sci.*, *149* (2020), Mar., ID106207
[14] Rehman, M. M. U., *et al.*, Numerical Investigation of Heat Transfer Enhancement and Fluid-flow Characteristics in a Micro-Channel Heat Sink with Different Wall-design Configurations of Protrusions Dimples, *Heat Mass Transf.*, *56* (2020), 1, pp. 239-255
[15] Derakhshanpour, K., *et al.*, Effect of Rib Shape and Fillet Radius on Thermal-hydrodynamic Performance of Micro-Channel Heat Sinks: a CFD Study, *Int. Commun. Heat Mass Transf., 119* (2020), Dec., ID104928
[16] Wang, G. L., *et al.*, Heat Transfer Enhancement in Micro-Channel Heat Sink with Bidirectional Rib, *Int. J. Heat Mass Transf.*, *136* (2019), June, pp. 597-609
[17] Khan, A. A., *et al.*, Performance Analysis of a Micro-Channel Heat Sink with Various Rib Configurations, *Journal Thermophys. Heat Transf.*, *70* (2016), 4, pp. 1-9
[18] Chai, L., *et al.*, Numerical Study of Laminar Flow and Heat Transfer in Micro-Channel Heat Sink with Offset Ribs on Sidewalls, *Appl. Therm. Eng.*, *92* (2016), Jan., pp. 32-41
[19] Xia, G. D., *et al.*, Optimum Thermal Design of Micro-channel Heat Sink with Triangular Reentrant Cavities, *Appl. Therm. Eng.*, *31* (2011), 6-7, pp. 1208-1219
[20] Ahmed, H. E., Ahmed, M. I., Optimum Thermal Design of Triangular, Trapezoidal and Rectangular Grooved Micro-Channel Heat Sinks, *Int. Commun. Heat Mass Transf.*, *66* (2015), Aug., pp. 47-57
[21] Kuppusamy, N. R., *et al.*, Heat Transfer Enhancement in a Micro-channel Heat Sink with Trapezoidal Cavities on the Side Walls, *Appl. Mech. Mate.*, *819* (2016), Jan., pp. 127-131
[22] Zhu, Q. F., *et al.*, Fluid-flow and Heat Transfer Characteristics of Micro-channel Heat Sinks with Different Groove Shapes, *Int. J. Therm. Sci.*, *161* (2021), Mar, ID 106721
[23] Kumar, P., Numerical Investigation of Fluid-Flow and Heat Transfer in Trapezoidal Micro-Channel with Groove Structure, *Int. J. Therm. Sci.*, *136* (2019), Feb., pp. 33-43
[24] Datta, A., *et al.*, A Conjugate Heat Transfer Analysis of Performance for Rectangular Micro-Channel with Trapezoidal Cavities and Ribs, *Int. J. Therm. Sci.*, *138* (2019), Apr., pp. 425-446
[25] Zhu, Q. F., *et al.*, Computational Study of rib Shape and Configuration for Heat Transfer and Fluid-Flow Characteristics of Micro-channel Heat Sinks with Fan-shaped Cavities, *Appl. Therm. Eng.*, *195* (2021), Aug., ID117171
[26] Qu, W., Mudawar, I., Experimental and Numerical Study of Pressure Drop and Heat Transfer in a Single-Phase Micro-Channel Heat Sink, *Int. J. Heat Mass Transf.*, *45* (2002), 12, pp. 2549-2565
[27] Webb, R. L., Performance Evaluation Criteria for Use of Enhanced Heat Transfer Surfaces in Heat Exchanger Design, *Int. J. Heat Mass Transf.*, *24* (1981), 4, pp. 715-726
[28] Steinke, M. E., Kandlikar, S. G., Single-phase Liquid Friction Factors in Micro-channels, *Int. J. Therm. Sci.*, *45* (2005), 11, pp. 1073-1083
[29] Phillips, R. J., Micro-Channel Heat Sinks, in: *Advances in Thermal Modelling of Electronic Components and Systems*, Hemisphere Publishing Corporation, New York, USA, 1990, pp. 84-109
[30] Chai, L., *et al.*, Heat Transfer Enhancement in Micro-Channel Heat Sinks with Periodic Expansion-Constriction Cross-sections, *Int. J. Heat Mass Transf.*, *62* (2013), July, pp. 741-751

Paper submitted: January 18, 2022
Paper revised: February 13, 2022
Paper accepted: February 28, 2022